EPJ Web of Conferences **239**, 01037 (2020) https://doi.org/10.1051/epjconf/202023901037
ND2019

Cross-section measurement in the reactions of ^{136}Xe on proton, deuteron and carbon

X. Sun[1,*], *H.* Wang[1], *H.* Otsu[1], *H.* Sakurai[1], *D.S.* Ahn[1], *M.* Aikawa[2], *N.* Fukuda[1], *T.* Isobe[1], *S.* Kawakami[3], *S.* Koyama[4], *T.* Kubo[1], *S.* Kubono[1], *G.* Lorusso[1], *Y.* Maeda[3], *A.* Makinaga[5,6,7], *S.* Momiyama[4], *K.* Nakano[8], *M.* Niikura[4], *Y.* Shiga[9,1], *P.-A.* Söderström[1], *H.* Suzuki[1], *H.* Takeda[1], *S.* Takeuchi[1], *S.* Taniuchi[4,1], *Ya.* Watanabe[1], *Yu.* Watanabe[8], *H.* Yamasaki[4], and *K.* Yoshida[1]

[1]RIKEN Nishina Center, 2-1 Hirowasa, Wako, Saitama 351-0198, Japan
[2]Faculty of Science, Hokkaido University, Sapporo 060-0810, Japan
[3]Faculty of Engineering, University of Miyazaki, Miyazaki 889-2192, Japan
[4]Department of Physics, University of Tokyo, 7-3-1 Hongo, Bunkyo, Tokyo 113-0033, Japan
[5]Graduate School of Medicine, Hokkaido University, Sapporo 060-8648, Japan
[6]JEin Institute for fundamental Science, NPO Einstein, Kyoto 606-8317, Japan
[7]Faculty of Fukuoka Medical Technology, Teikyo University, Fukuoka 836-8505, Japan
[8]Department of Advanced Energy Engineering Science, Kyushu University, 816-8580, Japan
[9]Department of Physics, Rikkyo University, Tokyo 171-8501, Japan

Abstract. The isotopic production cross sections for the reactions of ^{136}Xe induced by proton, deuteron and carbon at 168 MeV/u were obtained by using the inverse kinematics technique at RIKEN Radioactive Isotope Beam Factory. The target dependence of the cross sections was investigated systematically. It was found that for the light-mass products, the cross sections on carbon are larger than those on deuteron and proton. The measured cross sections on proton were compared with the previous data at higher reaction energies to study the energy dependence. The experimental results were compared with the theoretical calculations including both the intranuclear cascade and evaporation processes using PHITS and with the EPAX and SPACS empirical parameterizations.

1 Introduction

The spallation and fragmentation reaction play important roles in the production of the nuclei far from stability in radioactive beam facilities [1], which allow us to study the properties of both the proton-rich and neutron-rich nuclei. In addition, the spallation reaction has been considered as a promising mechanism for the nuclear waste transmutation. In recent years, the production cross sections of the proton- and deuteron-induced spallation reactions for the long-lived fission products (LLFPs) ^{137}Cs, ^{90}Sr [2], ^{107}Pd [3] and ^{93}Zr [4] were measured. For both of the two aspects, having a systematic understanding of the reaction mechanisms is of great importance and the cross section data are required .

For the stable nucleus ^{136}Xe, which is usually used as a primary beam, several experiments have been performed to study the spallation/fragmentation reactions. The production cross sections were measured for the proton-induced reactions at 1 GeV/u [5], 500 MeV/u [6], 200 MeV/u [7], and for the deuteron-induced reactions at 500 MeV/u [8] and beryllium-induced reactions at 1 GeV/u [9]. In order to investigate the energy dependence and target dependence for the cross sections of ^{136}Xe, we measured the cross sections for the reactions of ^{136}Xe + p, ^{136}Xe + d and ^{136}Xe + C at 168 MeV/u. These experimental results are fundamental data for the investigation of the reaction mechanism.

The isotopic distributions of the cross sections for ^{136}Xe induced by proton, deuteron and carbon at 168 MeV/u were obtained in the present work. The inverse kinematics was applied in the experiment by using the BigRIPS separator and the ZeroDegree spectrometer. By using the inverse kinematics technique, the reaction products were identified unambiguously and the target dependence can be investigated at the same reaction energy. The proton-induced cross sections were compared with the ones at 200, 500 and 1000 MeV/u to investigate the energy dependence.

2 Experiment

The experiment was performed at RIKEN Radioactive Isotope Beam Factory (RIBF), operated by RIKEN Nishina Center and the Center for Nuclear Study, University of Tokyo. The secondary beams were produced by the in-flight fission of a ^{238}U primary beam at 345 MeV/u bombarding on a beryllium target located at the entrance of the BigRIPS separator [10]. The particles in secondary beams

*e-mail: xhsun@pku.edu.cn

were identified in BigRIPS separator event by event using the TOF-$B\rho$-ΔE method [11]. The time of flight (TOF), the magnetic rigidity ($B\rho$) and the energy loss (ΔE) were measured to deduce the atomic number Z and the mass-to-charge ratio A/Q.

The inverse kinematics was adopted in the present experiment. The CH_2 (179.2 mg/cm^2), CD_2 (217.8 mg/cm^2) [12] and carbon (226.0 mg/cm^2) targets were used to induce the secondary reactions. In order to subtract the background contribution, the data by using the target frame without target material (empty target) were taken. The energy of ^{136}Xe was 168 MeV/u at the center of the secondary target, with the average intensity of 2.6×10^3 particles per second (pps). The reaction products were analyzed by ZeroDegree spectrometer [10] and the particle identification was made in a similar way to BigRIPS separator, by using the TOF-$B\rho$-ΔE method. In order to cover a broad range of the reaction products, 5 different $B\rho$ settings (+3%, 0%, -3%, -6%, -9%) were applied to the ZeroDegree spectrometer.

A particle identification plot in ZeroDegree spectrometer for the products produced from ^{136}Xe on CD_2 target with $B\rho$ -9% setting was shown in Fig. 1. The typical A/Q and Z resolutions were 6.1×10^{-3} (FWHM) and 0.52 (FWHM), respectively. For the reactions on CD_2 target, after the particles pass through the ZeroDegree spectrometer, the ratio of the fully-stripped ions ($Q = Z$) was about 66% for the xenon isotopes.

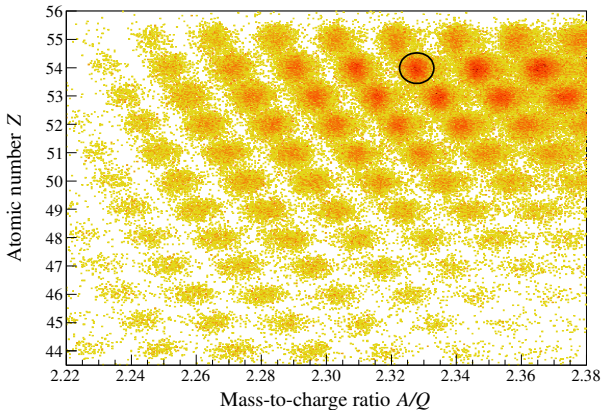

Figure 1. A particle identification plot of Z verse A/Q for the products produced from ^{136}Xe on CD_2 target with $B\rho$ -9% setting. The black circle indicates the ^{126}Xe to guide the eye.

3 Results and discussion

The isotopic distributions of the cross sections for the products produced by ^{136}Xe on proton, deuteron and carbon at 168 MeV/u are shown in Fig. 2. The cross sections on carbon (σ_C) were obtained from the data on carbon target after subtracting the background contribution from the empty target. The cross sections on proton (σ_p) and deuteron (σ_d) were obtained from the data on CH_2 and CD_2 targets, respectively, after subtracting the contributions from the carbon target and empty target. The statistical uncertainties were shown in Fig. 2. The systematic uncertainties originate from the contributions in the target thickness (less than 2%), the charge state distribution (less than 5%) and the acceptance in the ZeroDegree spectrometer (less than 10% for low-momentum products).

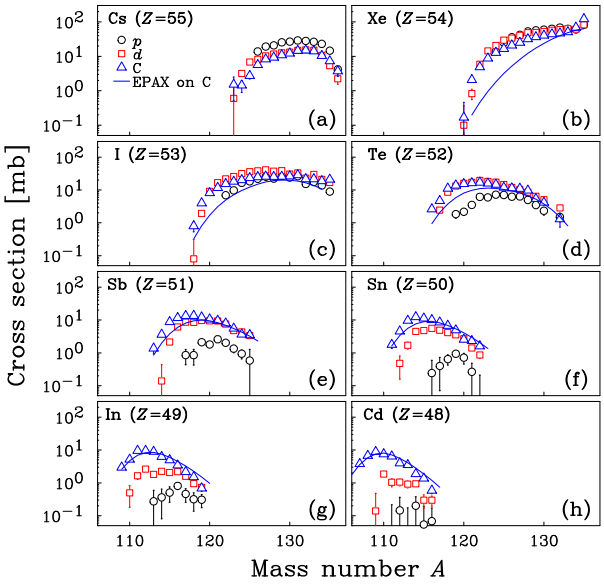

Figure 2. Isotopic distribution of the cross sections for ^{136}Xe on proton (circle), deuteron (square) and carbon (triangle) at 168 MeV/u. The error bars correspond to the statistical uncertainties. The solid line represents the EPAX calculations for the reactions on carbon.

For the cesium isotopes produced by the charge pickup reactions, the σ_p is larger than both the σ_d and σ_C, as shown in Fig. 2(a). The larger cross sections on proton than those on deuteron for charge pickup reactions were also found for ^{137}Cs at 185 MeV/u [2] and ^{107}Pd at 118 MeV/u [3]. For the xenon and iodine isotopes in Fig. 2(b) and 2(c), the cross sections keep almost constant over a wide mass range and then the cross sections gradually decrease towards the neutron-deficient side. These products are produced mainly from the peripheral reactions [9], where the evaporation process is dominated by the neutron evaporation. For other elements from tellurium to cadmium, the isotopic distributions show a bell shape. For these products, σ_p becomes smaller than σ_d and σ_C, especially for the isotopes in the neutron-deficient side. These light-mass products are produced by the central collision, where the production cross sections mainly dependend on the excitation energy of the pre-fragments. Since the number of nucleons is larger for carbon and deuteron than that of proton, the relatively higher energy can be deposited in the carbon- and deuteron-induced reactions. Therefore, σ_d and σ_C become larger than σ_p.

The cross sections on carbon measured in the present work were compared with the calculations by EPAX empirical parameterization [16], as shown in Fig. 2. In general, EPAX calculations reproduce the experimental re-

sults well, especially for the elements with atomic number $Z < 52$. Underestimation by EPAX was found in the neutron-deficient side of the xenon, iodine and tellurium isotopic chain. It is noted that the cross sections for cesium isotopes can not be calculated by EPAX.

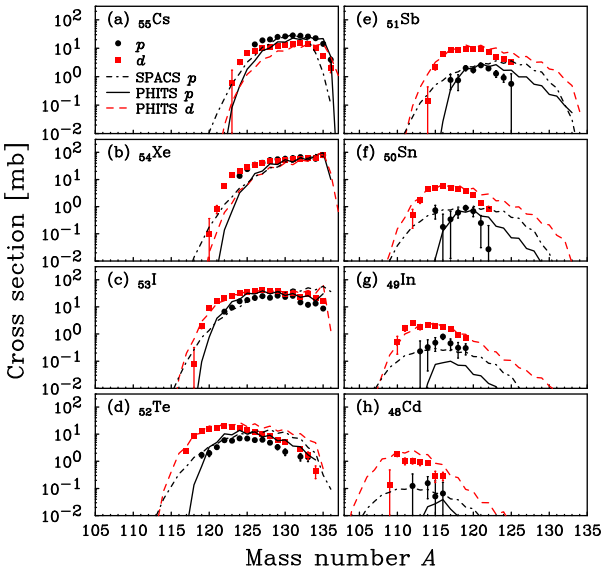

Figure 3. Isotopic distributions of the cross sections for the products that are produced in the reactions of ^{136}Xe + p (circle), ^{136}Xe + d (square) at 168 MeV/nucleon. The solid and dashed lines correspond to the PHITS calculations on proton and deuteron, respectively. The dot-dashed lines correspond to the SPACS [17] calculations on proton.

The comparison between the measured cross sections on proton and deuteron with the model calculations using Particle and Heavy Ion Transport system (PHITS) 2.76 [13] are shown in Fig. 3. The intranuclear cascade model of Liège (INCL) [14] and GEM [15] were used in PHITS calculations for the intranuclear cascade and evaporation processes, respectively. The PHITS calculations reproduced the experimental data for both the proton- and deuteron-induced reactions. PHITS underestimated the cross sections on the neutron-deficient side of cesium and xenon isotopic chain, which can be found in Fig. 3(a) and 3(b). The overestimation by PHITS was observed for the neutron-rich side of tellurium, antimony and tin, as shown in Fig. 3(d)-(f). For ^{135}Xe and ^{135}I that are produced by one-nucleon removal, PHITS calculations overestimated the cross sections. Similar results were also found for ^{93}Zr at 105 MeV/nucleon [4]. The calculations by SPACS semi-empirical parameterization [17] were also plotted in Fig. 3 to compared with the cross sections on proton. The SPACS calculations reproduced the trend of the experimental data on proton overall, while it was found that the SPACS calculations underestimate the cross sections for the neutron-deficient side of xenon isotopes in Fig. 3(b) and overestimate the cross sections in the neutron-rich side for iodine, tellurium, antimony and tin isotopes, as shown in Fig. 3(c)-(f).

The energy dependence for the proton-induced cross sections was studied by comparing the measured cross sections in the present work at 168 MeV/u with the results obtained previously at higher reaction energies. As shown in Fig. 4, the production cross sections at 200 MeV/u [7] (diamond) , 500 MeV/u [6] (square), and 1000 MeV/u [5] (circles) were plotted for comparison. For the charge pickup reactions in Fig. 4(a), the shape of the isotopic distribution is similar at different reaction energies, and the value of the cross sections decrease as the reaction energy increase. Such behavior for this reaction channel was also observed in the studies for ^{107}Pd [3]. The energy dependence for xenon isotopes was found in a similar minor as cesium isotopes, except the production of ^{135}Xe, for which the difference of the cross sections at different reaction energies is very small. For the elements with atomic number $Z < 54$ in Fig. 4 (c)-(h), the coverage of the isotopic distribution is wider at higher reaction energy. For the iodine and tellurium isotopes, the cross sections are larger at higher reaction energy in the neutron-deficient side, and the cross sections at 200 and 168 MeV/u decrease rapidly. As discussed above, for the antimony, tin, indium and cadmium elements, which are produced by central collision, the cross sections depend on the energy deposited in the pre-fragment. At higher reaction energy, more energy deposited during the cascade stage, resulting in a large production cross sections for the light-mass products by evaporating more nucleons.

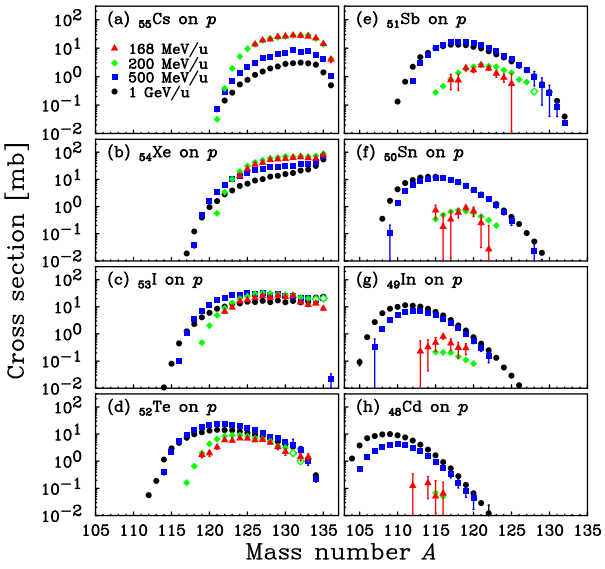

Figure 4. Comparison for the isotopic production cross sections of the proton-induced reactions at different reaction energies. The red triangles represent cross sections obtained in the present work at 168 MeV/nucleon. The green diamonds, blue squares and black dots represent the cross sections at 200 MeV/nucleon [7], 500 MeV/nucleon [6] and 1 GeV/nucleon [5], respectively. The open points at 200 MeV/nucleon represent the extrapolated values [17].

4 Summary

The isotopic distribution of the cross sections for ^{136}Xe on proton, deuteron and carbon at 168 MeV/u were ob-

tained in inverse kinematics technique at RIKEN Radioactive Isotope Beam Factory. The target dependence of the cross sections was investigated systematically. The cross sections of the light-mass products are found to be larger for the carbon-induced reaction because of the higher deposited energy. The cross sections for the proton-induced reactions obtained in the present work were compared with the previous data at higher reaction energies. It was found that the cross sections for cesium isotopes decrease as the reaction energy increase. The experimental results were compared with several calculations, PHITS, EPAX and SPACS. The overall tendency of the isotopic cross sections was reproduced by all these calculations. The comparison of the experimental data with the model calculations is expected to be helpful for the model benchmarking.

We express our gratitude to the accelerator staff of the RIKEN Nishina Center for providing the ^{238}U primary beam. This work was supported by the ImPACT Program of the Council for Science, Technology and Innovation (Cabinet Office, Government of Japan).

References

[1] H. Suzuki et al., Nucl. Instrum. Methods Phys. Res B **317**, 756 (2013)
[2] H. Wang et al., Phys. Lett. B **754**, 104 (2016).
[3] H. Wang et al., Prog. Thero. Exp. Phys. **2017**, 021D01 (2017).
[4] S. Kawase et al., Prog. Thero. Exp. Phys. **2017**, 093D03 (2017).
[5] P. Napolitani et al., Phys. Rev. C **76**, 064609 (2007).
[6] L. Giot et al., Nucl. Phys. A **899**, 116 (2013).
[7] C. Paradela et al., Phys. Rev. C **95**, 044606 (2017).
[8] J. Alcántara-Núñez et al., Phys. Rev. C **92**, 024607 (2015).
[9] J. Benlliure et al., Phys. Rev. C **78**, 054605 (2008).
[10] T. Kubo et al., Prog. Theor. Exp. Phys. **2012**, 03C003, (2012).
[11] N. Fukuda et al., Nucl. Instrum. Methods Phys. Res B **317**, 323 (2013).
[12] Y. Maeda et al., Nucl. Instrum. Methods Phys. Res A **490**, 518 (2002).
[13] T. Sato et al., J. Nucl. Sci. Technol. **50**, 913 (2013).
[14] A. Boudard et al., Phys. Rev. C **87**, 014606 (2013).
[15] S. Furihata, Nucl. Instrum. Methods Phys. Res. B **171**, 251 (2000).
[16] K. Sümmerer et al., Phys. Rev. C **61**, 034607 (2000).
[17] C. Schmitt et al., Phys. Rev. C **90**, 064605 (2014).